Molecular Cell
Article

Asymmetric Activation of the Hsp90 Dimer by Its Cochaperone Aha1

Marco Retzlaff,[1,3,4] Franz Hagn,[1,3] Lars Mitschke,[1] Martin Hessling,[1] Frederik Gugel,[1] Horst Kessler,[1,2] Klaus Richter,[1] and Johannes Buchner[1,*]
[1]Center for Integrated Protein Science Munich at the Department Chemie, Technische Universität München, D-85747 Garching, Germany
[2]Institute for Advanced Study, Technische Universität München, D-85747 Garching, Germany
[3]These authors contributed equally to this work
[4]Present address: Department of Biology and BioX Program, E200A James Clark Center, 318 Campus Drive, Stanford University, Stanford, CA 94305-5430, USA
*Correspondence: johannes.buchner@ch.tum.de
DOI 10.1016/j.molcel.2010.01.006

SUMMARY

The chaperone Hsp90 is an ATP-dependent, dimeric molecular machine regulated by several cochaperones, including inhibitors and the unique ATPase activator Aha1. Here, we analyzed the mechanism of the Aha1-mediated acceleration of Hsp90 ATPase activity and identified the interaction surfaces of both proteins using multidimensional NMR techniques. For maximum activation of Hsp90, the two domains of Aha1 bind to sites in the middle and N-terminal domains of Hsp90 in a sequential manner. This binding induces the kinetically unfavored N terminally dimerized state of Hsp90, which primes for the hydrolysis-competent conformation. Surprisingly, this activation mechanism is asymmetric. The presence of one Aha1 molecule per Hsp90 dimer is sufficient to bridge the two subunits and to fully stimulate Hsp90 ATPase activity. This seems to functionalize the two subunits of the Hsp90 dimer in different ways, in that one subunit can be used for conformational ATPase regulation and the other for substrate protein processing.

INTRODUCTION

The molecular chaperone Hsp90 is an ATP-driven machine that is crucial for the activation and structural maturation of its substrate proteins, including signaling kinases, transcription factors, and several unrelated proteins such as viral coat proteins (Geller et al., 2007; McClellan et al., 2007; Picard, 2002; Pratt and Toft, 2003; Prodromou and Pearl, 2003; Xu et al., 2005). The binding and hydrolysis of ATP are thought to provide the energy that drives the chaperone cycle. It is evident from biochemical and structural analysis that, during this cycle, Hsp90 undergoes large conformational changes (Ali et al., 2006; Dollins et al., 2007; Graf et al., 2009; Hessling et al., 2009; Mickler et al., 2009; Neckers et al., 2009; Richter et al., 2008; Shiau et al., 2006).

Hsp90 is a dimeric protein with an N-terminal nucleotide-binding pocket, a middle domain that is known to act as a discriminator between Hsp90 substrates (Hawle et al., 2006), and a C-terminal dimerization domain. The two N-terminal nucleotide-binding sites bind ATP independently (Richter et al., 2001). The changes induced in the N-terminal domain upon ATP binding ultimately lead to an N terminally dimerized conformation (Prodromou et al., 2000; Richter et al., 2002) and to a closed state that is active in ATP hydrolysis. After ATP turnover, the open state is restored again. In eukaryotes, accessory factors (so-called cochaperones) have been identified, which regulate the ATP turnover, induce structural changes in Hsp90, or are involved in the substrate activation process (Forafonov et al., 2008; Johnson et al., 1994, 1996; Pirkl and Buchner, 2001; Riggs et al., 2003; Siligardi et al., 2004). One of the inhibitors, p23/Sba1, binds preferentially to the N terminally closed, nucleotide-bound state (Ali et al., 2006; McLaughlin et al., 2006; Richter et al., 2004; Sullivan et al., 2002), whereas the cochaperone Hop/Sti1 binds to the open conformation of Hsp90, the putative resting state (Onuoha et al., 2008; Richter et al., 2003). Hop/Sti1 appears to use two binding sites to prevent the N-terminal closing of the two subunits and inhibits ATP hydrolysis completely in a noncompetitive manner (Richter et al., 2003). So far, only one known activator of the Hsp90 ATPase has been identified. In yeast, there are two different isoforms, Aha1 and Hch1. Hch1 was characterized as a high copy Hsp90 suppresser of a temperature-sensitive Hsp90 mutant in *Saccharomyces cerevisiae* (Nathan et al., 1999). Hch1 shares high-sequence homology to the N-terminal part of the *S. cerevisiae* protein Aha1 (activator of Hsp90 ATPase1). Homologs for Aha1 have been identified from yeast to mammals; in contrast, Hch1 is only encoded in the genomes of lower eukaryotes (Lotz et al., 2003; Panaretou et al., 2002). Aha1 has been implicated in a vast set of cellular processes, including the quality control of the cystic fibrosis transmembrane conductance regulator (CFTR) (Wang et al., 2006), the activation of v-Src and glucocorticoid receptors (Holmes et al., 2008; Lotz et al., 2003; Panaretou et al., 2002), and the phosphorylation status of signal transduction proteins (Holmes et al., 2008). Of note, overexpression of Aha1 was shown to inhibit the regulation function of Hsp90 in CFTR folding and export (Wang et al., 2006). A crystal structure of the middle domain of Hsp90 in complex

with the N-terminal domain of Aha1 shows that subtle changes occur in the middle domain involving the catalytic Arg380, which might be responsible for the activation of Hsp90 (Meyer et al., 2004). However, the lack of structural details of the entire Aha1 protein in complex with the Hsp90 dimer precludes a clear statement regarding the mechanism causing the strong stimulation of ATP hydrolysis. Here, we address this issue using a combination of biochemical and nuclear magnetic resonance (NMR) experiments together with Hsp90 and Aha1 mutants. We show that acceleration of the Hsp90 ATPase cycle requires the interaction of both domains of Aha1 in a cooperative manner with both the N-terminal and middle domains of Hsp90 in an asymmetric activation mechanism.

RESULTS

Aha1 Binds Preferentially to a Closed Hsp90 Dimer

Aha1 has been reported to strongly stimulate Hsp90 ATPase activity (Panaretou et al., 2002; Richter et al., 2008). A crystal structure of the middle domain of Hsp90 in complex with the N-terminal domain of Aha1 (Meyer et al., 2004) showed only minor changes in the activation loop of Hsp90 (amino acids 375–381). However, the mechanistic aspects of this interaction have not been addressed in the context of the full-length protein. To analyze the binding of yeast Aha1 to yeast Hsp90, we used wild-type Hsp90 (Hsp90 WT) and a well-characterized Hsp90 mutant, Δ8-Hsp90, which lacks eight amino acids at the N-terminal end. This mutant could serve as a conformational probe because it adopts the closed conformation in response to ATP more readily than Hsp90 WT (Richter et al., 2002). We found that Aha1 binds more tightly to Δ8-Hsp90 than to Hsp90 WT (K_D = 1.2 versus 3.8 μM) and that the maximum stimulation of ATPase activity is reduced in the mutant (v_{max} = 4.2 min^{-1} for Δ8-Hsp90 versus 15.3 min^{-1} for Hsp90 WT) (Figure S1 available online). Given that Δ8-Hsp90 is trapped in the closed conformation after ATP addition, our data imply that Aha1 induces and preferentially binds to the closed conformation of Hsp90.

Aha1 Binding to Hsp90 Involves Both Domains of Aha1

It is difficult to reconcile the observed conformation-sensitive interaction of Aha1 and Hsp90 with Aha1 binding solely to Hsp90s middle domain. To address the role of the individual domains of Aha1 in the activation mechanism, we divided the cochaperone into two parts according to its domain structure (Meyer et al., 2004). The N-terminal domain corresponds to the protein Hch1, indicating that this part of Aha1 is a functional domain by itself. Both domains (termed Aha1-N and Aha1-C) (Figure 1A) are stable proteins, as analyzed by circular dichroism spectroscopy and thermal denaturation curves (Figure S2 and Table S1). Aha1 and each of the fragments are monomeric in solution, and no complex formation of the individual domains could be detected (data not shown).

We tested whether Aha1-N or Aha1-C could stimulate the ATPase activity of Hsp90 WT (Figure 1B). Whereas Aha1-C had no effect on the ATP turnover rate (k_{cat}), Aha1-N accelerated it; however, the stimulation was reduced 10-fold compared to the full-length wild-type protein (Figure 1B, inset), consistent

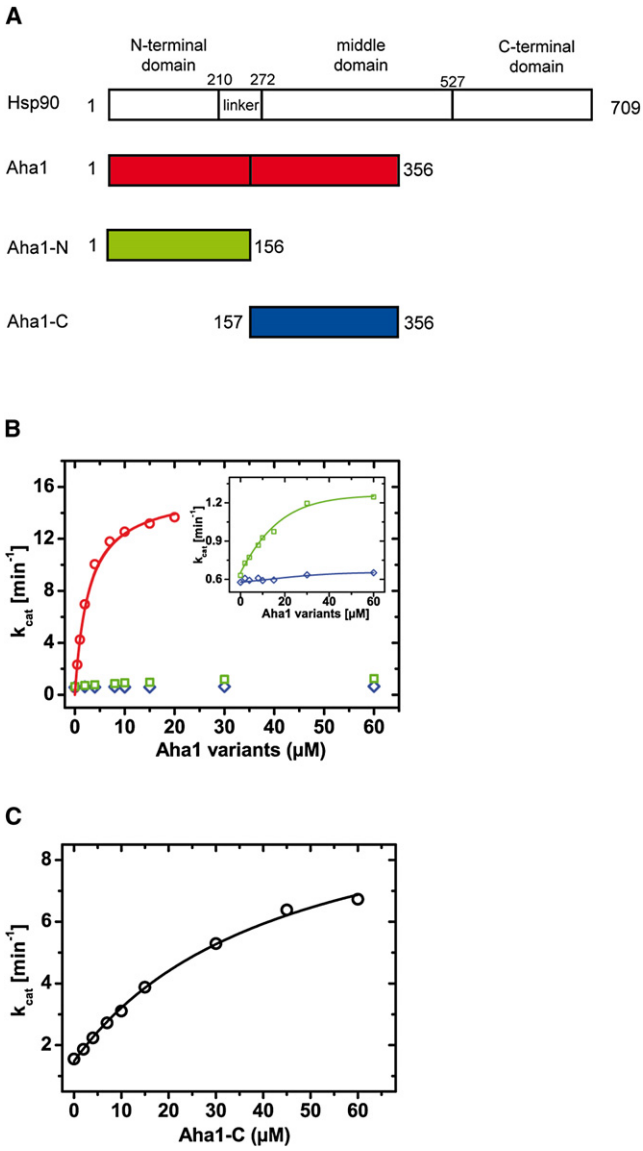

Figure 1. Effects of Aha1 and Aha1 Domains on the ATPase Activity of Hsp90

(A) Schematic showing domain organization of the yeast proteins yHsp90 and yAha1. Aha1 was subdivided into the N-terminal domain, Aha1-N, and the C-terminal domain, Aha1-C.

(B and C) Assays were performed at 30°C in 40 mM HEPES/KOH (pH 7.5), 20 mM KCl, 10 mM $MgCl_2$, and 5 mM ATP and corrected for background activity using 125 μM radicicol. Data were fit according to equation 1. In the absence of Hsp90, Aha1 and Aha1 fragments show no ATPase activity (data not shown).

(B) Stimulatory effect of Aha1 (red), Aha1-N (green), and Aha1-C (blue) on the ATPase activity of Hsp90. 1 μM Hsp90 was incubated with Aha1 or Aha1 fragments in concentrations ranging from 0–60 μM prior to the ATPase assay. (Inset) Enlarged view of Aha1-N and Aha1-C results.

(C) 60 μM Aha1-N was preincubated with 1 μM Hsp90. The Aha1-C fragment was titrated to the complex in a concentration range of 0–60 μM, and the effect on the ATPase activity of Hsp90 was measured as in (B).

with previous reports (Panaretou et al., 2002). The affinity of Aha1-N for Hsp90 was also reduced (K_D = 19 μM compared to 3.8 μM for wild-type Aha1). Of interest, titrating Aha1-C to

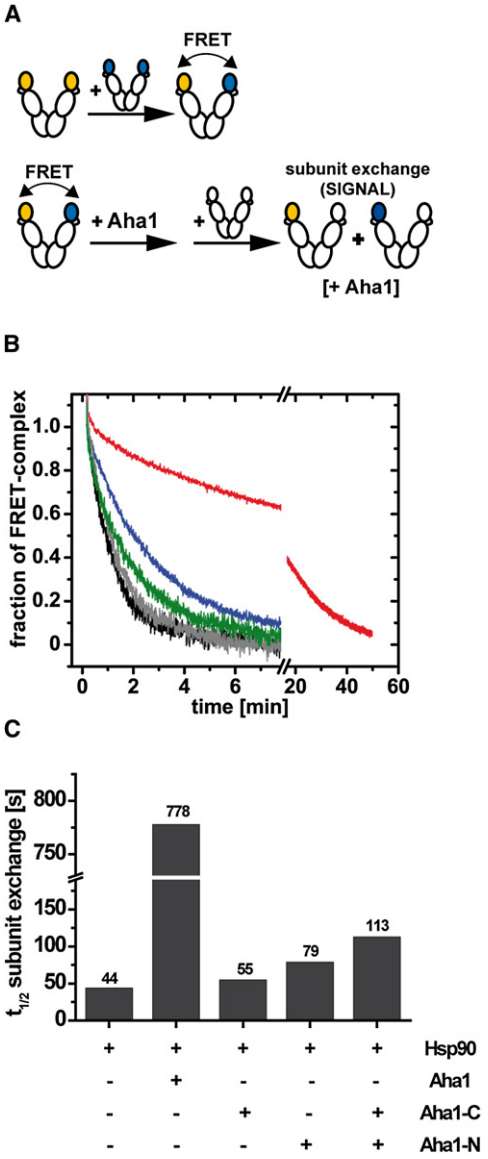

Figure 2. Binding of Aha1 and Aha1 Domains and the Bridging Function of Aha1 Visualized by Fluorescence Resonance Energy Transfer

(A) Scheme of fluorescence resonance energy transfer (FRET) experiments. Donor- and acceptor-labeled Hsp90 were incubated to allow subunit exchange and the formation of FRET-competent heterodimers (top). Aha1 was then added to the preformed heterodimers (bottom). After complete complex formation, the formed Aha1 containing Hsp90 FRET complexes were chased by the addition of a large excess of unlabeled Hsp90, which leads to a disassembly of the formed complex, as seen in (B). The rates of this Hsp90 subunit exchange rely on the stability of Hsp90 protomer association.

(B) Subunit exchange of 200 nM Hsp90 heterodimers in the absence or presence of Aha1 or individual Aha1 domains after the addition of 10 μM unlabeled Hsp90 WT. Shown is the normalized decrease of Hsp90 acceptor fluorescence over time and the effect of Aha1 (20 μM, red), Aha1-N (60 μM, green), Aha1-C (60 μM, gray), or a 1:1 mixture of Aha1-N and Aha1-C (120 μM, blue).

(C) The apparent half-life ($t_{1/2}$) of each subunit exchange reaction of Hsp90 dimers is derived from the FRET experiments shown in (B). The qualitative half-life in the absence or presence of Aha1 variants was estimated as described in the Experimental Procedures, equation 2.

a preformed complex of Hsp90 and Aha1-N partially restored the stimulation potential, bringing it closer to that of wild-type Aha1 (Figure 1C). These results point toward at least two cooperative binding sites for Aha1 in Hsp90, with the activation potential of the Aha1 C-terminal domain depending strongly on the presence of Aha1-N.

Aha1 Stabilizes the ATPase-Competent Hsp90 Dimer

The activation mechanism of Aha1 implies a complex binding mode that includes contributions of the individual Aha1 domains and results in N-terminal association of Hsp90. We used Förster resonance energy transfer (FRET) of labeled Hsp90 dimers (Hessling et al., 2009) to study the effects of Aha1 on the subunit exchange of the Hsp90 dimer (Figure 2A). FRET-competent Hsp90 heterodimers were treated with Aha1 or the individual Aha1 domains. The stability of each of the Aha1-Hsp90 FRET complexes was addressed by a chase with an excess of unlabeled Hsp90 WT (Hessling et al., 2009). The disassembly of the FRET complex could be monitored by a decrease in the Hsp90 acceptor fluorescence (Figure 2B). These data were analyzed by single exponentials to determine the apparent half-life of the reaction (Figure 2C). In the presence of Aha1, the half-life of the Hsp90 subunit exchange reaction was increased 20-fold compared to its half-life in the absence of Aha1. Thus, Aha1 binding resulted in a stronger association of the two Hsp90 subunits, even in the absence of nucleotides. The individual Aha1 domains failed to stabilize the Hsp90 dimer; however, the presence of both Aha1 domains resulted in a moderate effect on the Hsp90 subunit exchange rate (Figures 2B and 2C).

Thus, Aha1 seems to coordinate the domains in the Hsp90 dimer, thereby stabilizing the ATPase-competent conformation of the Hsp90 dimer.

Aha1 Activation Stimulates the Hsp90 Subunits in Both *Cis* and *Trans*

To decipher the underlying mechanism of Aha1 function, we created Hsp90 heterodimers in which the middle domain of one of the subunits was mutated to disrupt Aha1 binding. For this purpose, we chose the Hsp90V391E mutant, as V391 participates in the interaction of Aha1-N with the middle domain of Hsp90 (Meyer et al., 2004). To prove that binding of Aha1 to Hsp90V391E is disrupted, we developed an analytical ultracentrifugation assay to detect the binding of FITC-labeled Aha1 to Hsp90 (Figure S3A). We found that the ability of Aha1 to bind to Hsp90V391E was strongly reduced compared to Hsp90 WT. As expected, the Hsp90V391E variant required at least 50-fold higher concentrations of Aha1 for stimulation (Figure S3B), implying that the interaction was successfully disrupted. In addition, we generated the ATPase-inactive mutant Hsp90D79N, which is not able to bind or hydrolyze ATP (Obermann et al., 1998; Panaretou et al., 1998), and the double mutant Hsp90V391E/D79N, which cannot bind Aha1 (Figure S3A) in addition to not being able to bind or hydrolyze ATP. As expected, in the absence of Aha1, the Hsp90 variants carrying the D79N

All experiments were performed in 40 mM HEPES/KOH (pH 7.5) and 20 mM KCl at 20°C.

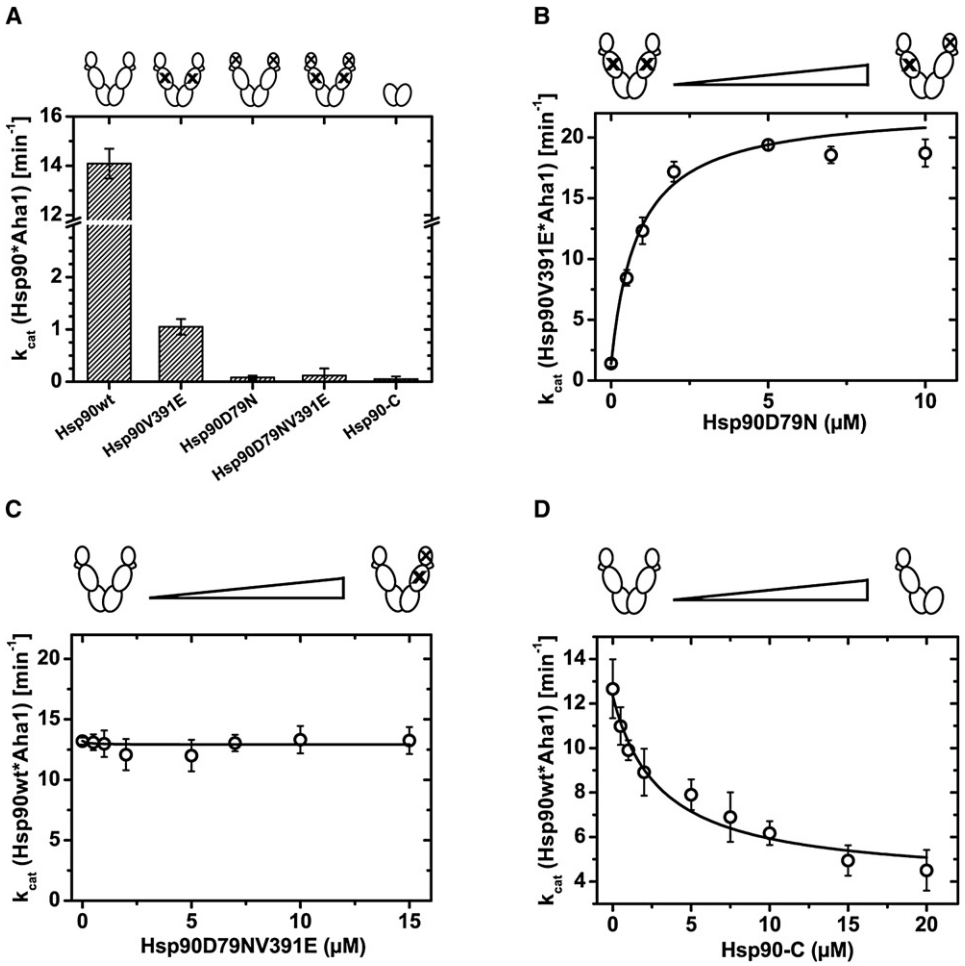

Figure 3. Heterodimer ATPase Assay to Visualize the Activation Mechanism of Aha1

(A) Steady-state k_{cat} values of 1 μM Hsp90 WT and mutants in the presence of 10 μM Aha1.

(B–D) Effect of heterodimer formation on the Aha1-stimulated ATPase activity of Hsp90. Heterodimer formation is visualized schematically on top of each graph, starting with the Hsp90 homodimer as indicated in (A) and ending with the ATPase-active heterodimeric Hsp90 species of interest. Heterodimer formation was achieved by mixing Hsp90 variants and incubating at 30°C for 10 min before adding Aha1 and incubating for an additional 5 min.

(B) ATPase activity of 1 μM Hsp90V391E in the presence of 10 μM Aha1 and increasing concentrations of Hsp90D79N.

(C) ATPase activity of 1 μM Hsp90 WT in the presence of 10 μM Aha1 and increasing concentrations of the double-mutant Hsp90D79NV391E.

(D) ATPase activity of 1 μM Hsp90 WT in the presence of 10 μM Aha1 and increasing concentrations of the Hsp90 C-terminal domain.

Data were fit according to equation 1; error bars indicate standard deviation. ATPase assays were performed in 40 mM HEPES/KOH (pH 7.5) and 20 mM KCl at 30°C.

mutation were devoid of ATPase activity, whereas the variant Hsp90V391E exhibited normal ATP hydrolysis (data not shown). In the presence of Aha1, Hsp90V391E showed a dramatic reduction in Aha1-induced activation, correlating with a reduced binding affinity for Aha1; the Hsp90 variants carrying the D79N mutation again showed no ATPase activity (Figure 3A).

Using this set of mutants, we tested whether ATPase activity could be stimulated in the Hsp90 dimer subunit to which Aha1 is not bound. For the analysis of a *trans* activation, we used a constant concentration of Hsp90V391E (the mutant lacking Aha1 binding) and increasing concentrations of Hsp90D79N in the presence of Aha1. As expected, we found that, in the absence of Hsp90D79N, the ATPase activity of Hsp90V391E was not affected by Aha1 (Figure 3B). With increasing concentrations of Hsp90D79N, heterodimers predominate, which contain one subunit that has ATPase activity but cannot bind Aha1 and another subunit that can bind Aha1 but is inactive as an ATPase. Of interest, under these heterodimer conditions, we observed a 20-fold increase in the ATP turnover rate, demonstrating that the heterodimers were efficiently activated by Aha1. In the absence of Aha1, no significant changes were observed upon addition of Hsp90D79N (data not shown).

It should be noted that these data also conclusively show that Aha1 can bind to one subunit in the Hsp90 dimer and stimulate the ATPase in the other subunit, resulting in a stoichiometry of one Aha1 molecule per Hsp90 dimer. This stoichiometry is sufficient for the full activation potential of Aha1 in the Hsp90 dimer. We confirmed this stoichiometry using isothermal titration

calorimetry (ITC). We titrated Aha1 against Hsp90 WT and Hsp90D79N and observed identical binding curves (Figure S4A) with a stoichiometry of two Aha1 molecules per Hsp90 dimer, implying that, under full saturation, both subunits of Hsp90 bind Aha1. Given that our heterodimer experiment was performed with a binding capacity of only one Aha1 per Hsp90 dimer (due to the V391E mutation), we wanted to confirm that only one Aha1 molecule was bound to this construct. We generated Hsp90D79N/Hsp90V391E heterodimers by using a large excess of Hsp90V391E and titrated Aha1 to this mixture. The stoichiometry of Aha1 per Hsp90 heterodimer consisting of Hsp90D79N/Hsp90V391E was 1:1, implying that, indeed, one Aha1 molecule was bound per heterodimer (Figure S4A).

Next, we tested the possibility of a *cis* activation by Aha1. To this end, we used Hsp90 WT and inhibited the *trans* activation by forming heterodimers with the Hsp90D79N/V391E mutant (Figure 3C). Under heterodimer conditions, we observed a nearly unchanged ability of Aha1 to stimulate the Hsp90 ATPase activity, suggesting that *cis* activation also occurs. To exclude the possibility that we had failed to generate heterodimers, we tested the ability of Hsp90D79N/V391E to form heterodimers using a FRET-based Hsp90 subunit exchange assay. As shown in Figure S4B, this variant is clearly able to form heterodimeric Hsp90.

As a control, we used the Hsp90 C-terminal domain and formed heterodimers with Hsp90 WT. Under these conditions, ATP turnover decreased as the levels of Hsp90 C-terminal domain heterodimers increased (Figure 3D). These results suggest that the *cis* activation of Aha1 in the Hsp90 dimer requires the presence of two full-length protomers. However, one of them can be catalytically inactive. Thus, the stimulation of Hsp90 ATPase by Aha1 is possible in *cis* and *trans*, but surprisingly, neither seems to require two Aha1 proteins bound to the Hsp90 dimer.

Aha1 Binding to Hsp90 Involves the N-Terminal and Middle Domains of Hsp90

Binding of Aha1 leads to a stronger N-terminal dimerization and to stimulation of the hydrolysis reaction in both subunits. This scenario suggests an interaction of Aha1 with the middle domain and with at least one other binding site in Hsp90. To determine the interaction surfaces in the Aha1-Hsp90 complex at the resolution of individual residues, we performed multidimensional NMR experiments. We used the assignments of the N-terminal and middle domains of Hsp90 (Dehner et al., 2003; Salek et al., 2002) and performed chemical shift perturbation studies with isotope-labeled Hsp90. The titration of Aha1 to the labeled Hsp90 middle domain induced significant chemical shift perturbations at residues 357–361, 390–399, 457, 479, and 497 (Figure 4A, left). The binding site determined by these experiments reflects the interaction surface described in the crystal structure of the complex between the Hsp90 middle domain and Aha1-N (Meyer et al., 2004).

Having confirmed the binding site in the Hsp90 middle domain, we tested the interaction of the Aha1 constructs with the Hsp90 N-terminal domain. We observed chemical shift changes in the ^{15}N-labeled N-terminal domain in response to Aha1-N addition (Figure 4A, middle), leading to significant line broadening and chemical shift perturbations in the spectrum. These data imply that a specific interaction occurred. The responding peaks are localized at the first residues of helix 2 (residues 29–32) and in the last α helix and the C-terminal β strand (residues 187–210), suggesting that a second binding site for Aha1-N exists in the N-terminal domain. In the nucleotide-free form of the Hsp90 N domain, no significant chemical shift changes were detected upon addition of Aha1-C. However, in the AMP-PNP-bound form, the Hsp90 N domain showed specific binding of Aha1-C (Figure 4A, right). Chemical shift differences appear within helix 1 (residues 13–29), at the ATP lid region (residues 91–123), and at residue 197 in helix 7. In addition, residues in strands 5 and 6 (148–164) are also affected. These residues are located at the back side of the Hsp90 N-terminal domain. When full-length Aha1 is used, chemical shift differences appear at the same positions as with the individual Aha1 domains (data not shown). These results are in agreement with the idea that Aha1 binds preferentially to and stabilizes the closed Hsp90 complex. After mapping the involved amino acids in the full-length Hsp90 structure, a cluster is formed including both N-terminal domains (Figure 4B) forming a huge hydrophobic binding groove. The specific residues involved in binding include residues of the ATP lid and helix 1 and residues at the bottom of the ATP-binding pocket (D132, N151, and T157) in the Hsp90 N domain. The hydrophobic groove is likely formed by both N domains of the Hsp90 dimer (Figure 4B), which suggests that both Hsp90-N domains participate in the interaction with the Aha1 molecule.

To determine the interaction site on Aha1-C, we assigned 94% of all nonproline residues in the folded part (residues 213–350) of Aha1-C (Figure S5, top). Chemical shift and NOE analysis confirmed the location of secondary structure elements found in a homology model of the Aha1 C-terminal domain obtained from the human homolog (Protein Data Bank [PDB]:1x53) (Figure S5, bottom). NMR experiments in the presence of Hsp90 N and the ^{15}N-labeled Aha1-C domain showed that the interaction is enhanced, revealing stronger interactions in the presence of AMP-PNP (Figure 5A). The residues showing significant shifts are labeled in the chemical shift perturbation plot. Mapping of the amino acids involved in the interaction onto the homology model of the Aha1 C-terminal domain (Figure 5B) allowed us to describe the interaction surface on both proteins. The main areas affected by binding of the Hsp90 N-terminal domain are the Aha1-C β sheet region (residues L272, H284, and T297) at the bottom of the structure and the loop around residues H309 and E310.

Ternary Complex Formation of Aha1-Hsp90 with Hop/Sti1 or p23/Sba1

The integration of Aha1 into the scheme of Hsp90 cofactor complexes is still an open issue, and conflicting results have been reported in the past (Harst et al., 2005; Martinez-Yamout et al., 2006; Panaretou et al., 2002). For Hsp90-p23/Sba1 and Hsp90-Hop/Sti1 complexes, a competitive binding mode has been suggested (Richter et al., 2004). To analyze interactions within potentially ternary protein complexes, we formed a complex between Hsp90 and Sti1 at different Sti1 concentrations and determined the stimulatory effects of Aha1. In the

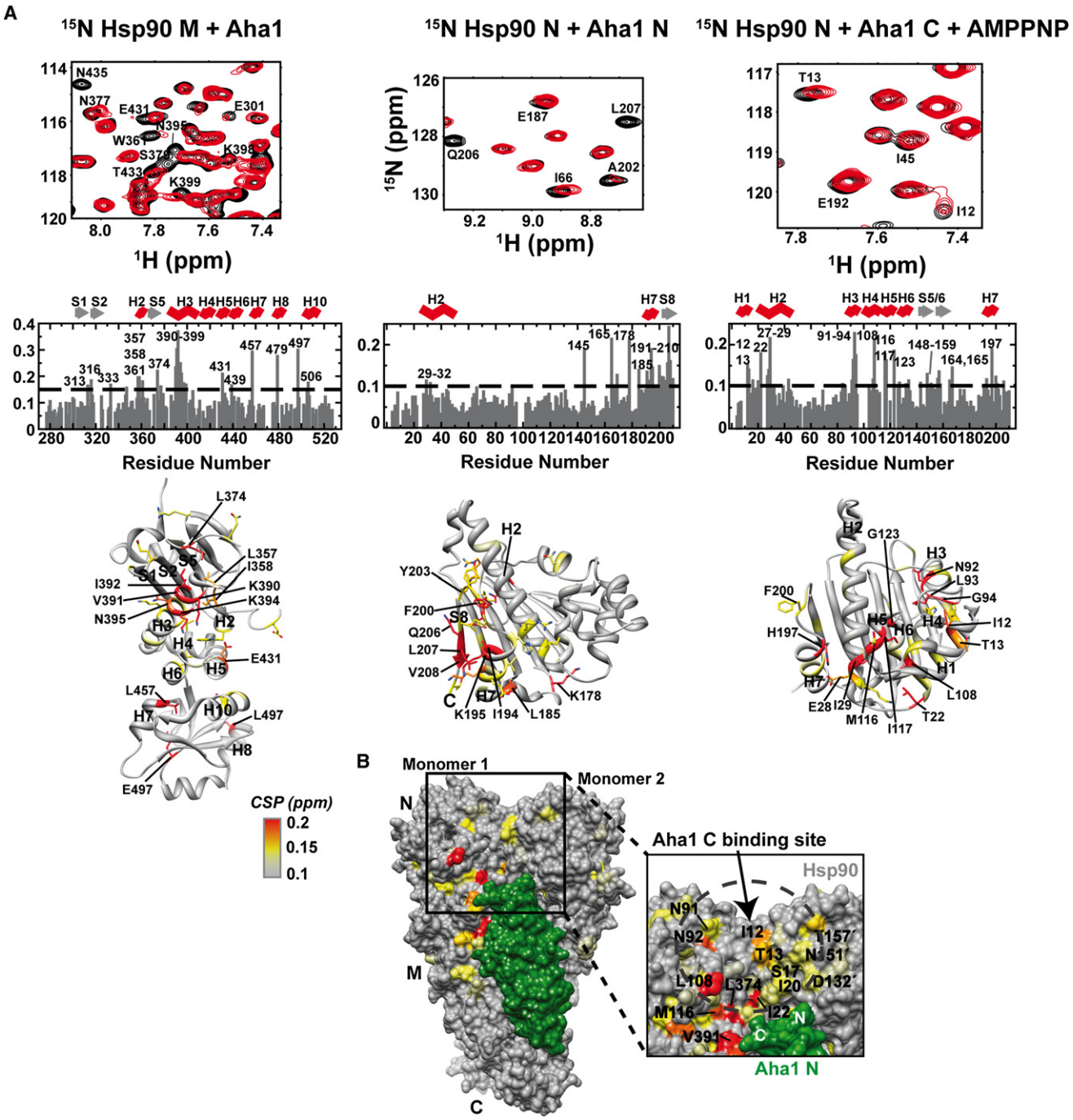

Figure 4. Determination of the Interaction Sites between Individual Domains of Hsp90 and Aha1

(A) Sections of ^{15}N-HSQC spectra of the Hsp90 middle domain (left) and the Hsp90 N-terminal domain (middle and right) in the presence of Aha1-N and Aha1-C (black, Hsp90 domain alone; red, in presence of Aha1 variants). Aha1-N interacts with the Hsp90 middle domain (left) and the Hsp90 N-terminal domain (center). Aha1-C interacts with the AMP-PNP-bound form of the Hsp90 N domain (right). The corresponding chemical shift perturbation (CSP) plots are shown below the ^{15}N-HSQC sections. CSPs were mapped onto the individual Hsp90 domains as shown in the structures below the plots (gray, not significant; yellow, significant; red, significant plus one standard error or above).

(B) Mapping of the chemical shift differences derived from (A) onto the dimeric Hsp90 full-length structure (PDB:2cg9) (CSP intensity increases from gray to red). The chemical shift differences within the Hsp90 middle domain (M) induced by Aha are in agreement with a crystal structure of the Hsp90 middle domain-Aha1 N domain complex (PDB:1usu). Therefore, Aha1-N (green) was docked to the full-length structure of Hsp90 using the known structure of the Hsp90 middle domain-Aha1-N complex. In addition, chemical shift differences appear at the Hsp90 N-terminal domain (N) either with Aha1-N or Aha1-C. Residues from both monomers contribute to the binding surface for Aha1 and are mapped onto the Hsp90 N domain. Significantly affected residues are labeled. The affected surface region within Hsp90 forms a large hydrophobic binding groove where Aha1-C binds, as indicated by the arrow.

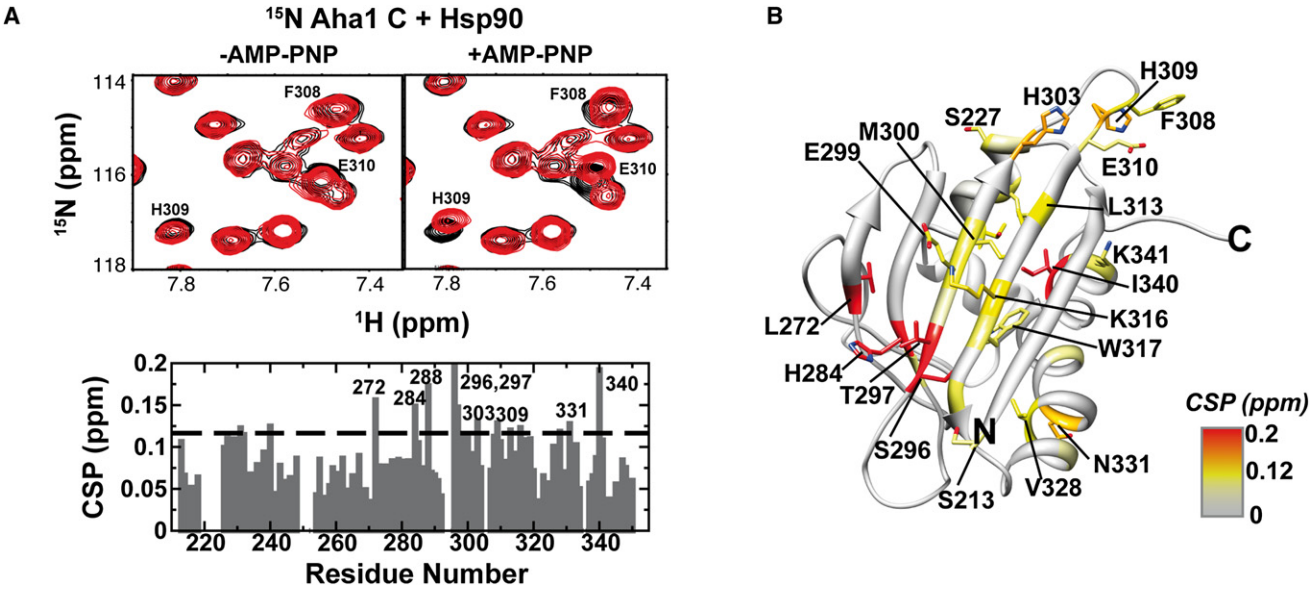

Figure 5. Determination of the Interaction Sites between Aha1-C and Hsp90

(A) Sections of a ^{15}N-HSQC spectra of Aha1-C without (black) and with (red) the Hsp90 N domain (see also Figure S4). Significant chemical shift changes appear only in the presence of the AMP-PNP-bound form of the Hsp90 N domain (right). The chemical shift plots for the whole protein are shown below, with significantly shifting residues in Aha1-C labeled.

(B) Averaged chemical shift differences derived from (A) mapped onto a homology model of Aha1-C based on the NMR structure of the human Aha1-C homolog (PDB:1x53) (CSP intensity increases from gray to red). Significant effects appear at the bottom of the β sheet region, which seems to be the main interaction interface with Hsp90-N.

presence of Sti1, the apparent K_D value of the Aha1-Hsp90 interaction increased from 3.8 to 32 μM (Figure 6A), and Sti1 limited the maximum stimulation rate at Aha1 saturation. These values suggest that both proteins have the potential to form ternary complexes, even though the interaction with Aha1 appears to be hindered by the presence of Sti1 to some extent.

To monitor the effect of Aha1 on the interaction of Hsp90 with p23/Sba1, we used the Δ8-Hsp90 mutant, which can be effectively inhibited in the presence of p23/Sba1 (Richter et al., 2004). We incubated different concentrations of p23/Sba1 with Δ8-Hsp90 and tested whether Aha1 could stimulate the ATPase activity. Similar to results obtained with the Hsp90-Sti1 complex, the binding affinity of p23/Sba1 was significantly increased (from 1.25 to 35 μM) (Figure 6B). On the other hand, the v_{max} observed in the presence of saturating concentrations of Aha1 was strongly reduced compared to results obtained in the absence of Sba1 (2.5 s^{-1} versus 4.2 s^{-1}), implying that these two cochaperones bind simultaneously to Hsp90, affecting each other's K_D values significantly.

DISCUSSION

Cochaperones regulate the cycle of Hsp90-client protein interactions in eukaryotes (Nathan et al., 1999; Pratt and Toft, 2003; Smith et al., 1993; Wandinger et al., 2006). However, exactly how cochaperones modulate the chaperone cycle of Hsp90 is far from clear. Here, we present a model for the activation mechanism of Aha1, the thus far unique ATPase-stimulating cochaperone of Hsp90. It should be noted that activators of ATPase activity have also been described for the Hsp70 chaperone system. Prominent examples are the Hsp40/DnaJ proteins (Bukau et al., 2006; Fan et al., 2003). These proteins have been shown to bind to Hsp70 and stimulate the ATP hydrolysis rate. However, the mechanism by which the Hsp40/DnaJ proteins affect the conformation of Hsp70 during this reaction is still unknown. For Aha1, our analysis indicates that it accelerates the Hsp90 ATPase by binding to the N-terminal and middle domains of the Hsp90 dimer and that it favors a specific conformation during the catalytic cycle of Hsp90. Although the yeast Aha1-N domain has some stimulation potential (Panaretou et al., 2002), both domains of Aha1 must act in a cooperative manner to achieve efficient activation of Hsp90. Our NMR experiments revealed that the binding of Aha1 to Hsp90 involves a region in the Hsp90 N-terminal domains in addition to the previously reported site in the Hsp90 middle domain (Meyer et al., 2004). Of interest, the Aha1-N domain binds to both the N-terminal and middle domains of Hsp90 in a nucleotide-independent manner. However, in our NMR experiments, the Aha1-C domain showed detectable binding to the N-terminal domain of Hsp90 only in the presence of nucleotides. In addition, we identified a binding site for the Aha1-N domain located in the C-terminal end of the Hsp90 N domain. This region partly contacts the Hsp90 middle domain, as seen in the ATP-bound full-length structure of Hsp90 (Ali et al., 2006). When the nucleotide-bound form of the Hsp90 N domain was incubated with the C-terminal domain of Aha1, the amino acids involved in this interaction could be localized mainly in the ATP lid and the first helix of Hsp90.

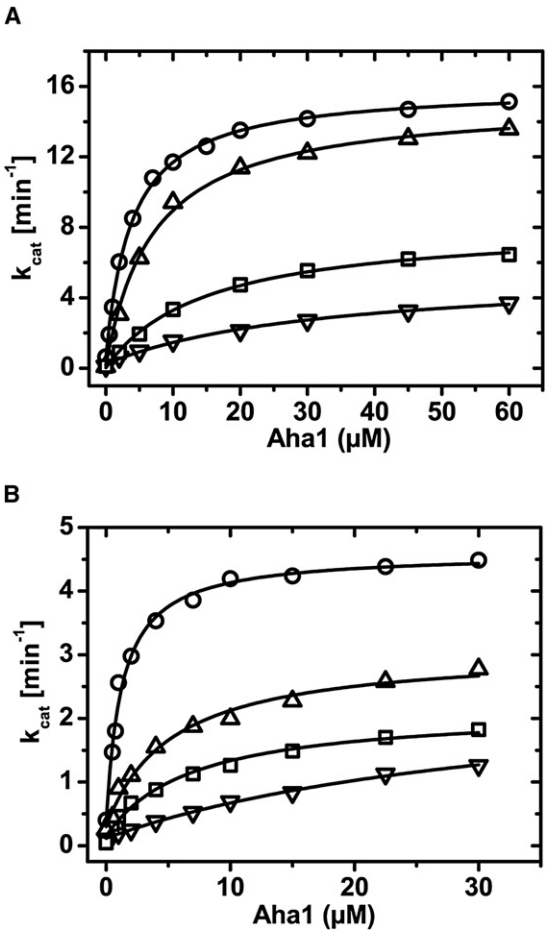

Figure 6. Influence of Regulatory Hsp90 Cochaperones Sba1 and Sti1 on the Stimulatory Effect of Aha1

(A) Four different concentrations of Sti1 (0 μM [O], 1 μM [Δ], 2 μM [□], and 4 μM [▽]) were incubated with 1 μM Hsp90 WT, and the influence of increasing concentrations of Aha1 was monitored by ATP hydrolysis in 40 mM HEPES/KOH, 20 mM KCl, 5 mM $MgCl_2$, and 5 mM ATP. Data analysis to determine the binding affinity of Aha1 and the v_{max} values were performed as described in the Experimental Procedures using equation 1.

(B) Four different concentrations of Sba1 (0 μM [O], 1 μM [Δ], 2 μM [□], and 4 μM [▽]) were used together with 1 μM Δ8-Hsp90, and the influence of increasing concentrations of Aha1 was monitored by ATP hydrolysis as in (A).

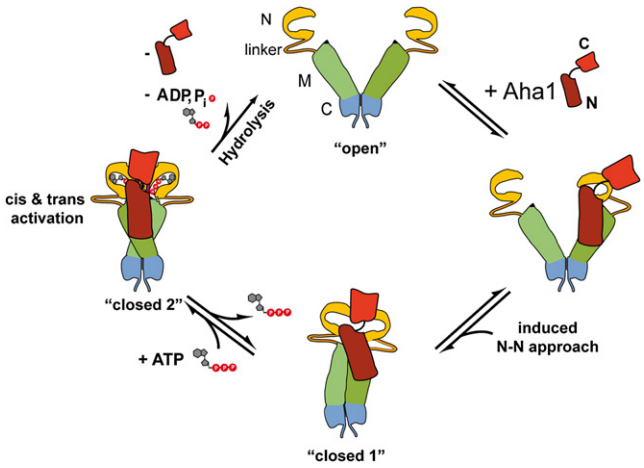

Figure 7. Schematic Representation of the Activation Mechanism of Aha1

One Aha1 molecule binds to the Hsp90 dimer, which is in the relaxed "open" state in an asymmetric manner. The Aha1 N-terminal domain serves as a primary binding domain and initializes complex formation, followed by a positioning of the Aha1 C-terminal domain. Binding of Aha1 induces a new domain orientation in Hsp90 in which the N-terminal nucleotide-binding domains are closer together (termed "closed 1"). ATP binding induces a second closed conformation ("closed 2"), which exhibits a higher affinity and an additional binding site for Aha1. The Aha1 C-terminal domain binds into a newly formed groove, contacting both Hsp90 N domains. One Aha1 molecule is sufficient to fully stimulate the activation of the Hsp90 ATP-binding domains in both *cis* and *trans*, thereby maintaining free binding sites for potential Hsp90 clients. After ATP turnover and release of ADP, Hsp90 returns to the "open" ground state.

We propose a model in which the Aha1 N domain is the primary binding domain and contributes substantially to complex formation. This model is supported by the finding that a mutation in the Aha1 N-terminal domain (D53K) shows a highly reduced Hsp90 stimulation potential (Meyer et al., 2004). Binding of the N domain of Aha1 seems to localize its C domain to the interaction site within the Hsp90 N-terminal domains. The Aha1-C domain may stabilize the large hydrophobic surface area within the Hsp90-N domain that is exposed during the dimerization reaction. This could lead to more rapid conformational changes on the way to the dimerized, closed state of Hsp90 and could consequently accelerate the ATPase activity, as the structural rearrangements leading to the closed state are the kinetically limiting steps of the Hsp90 ATPase cycle (Hessling et al., 2009). Thus, it seems that Aha1 induces a mechanical coupling of the middle and N-terminal domains of Hsp90, which allows the modulation of the structural rearrangements in the Hsp90 dimer and results in an increase in ATP turnover rate (Figure 7). This mechanism is further supported by our FRET experiments showing that binding of Aha1 stabilizes the ATPase-competent state by bridging the two Hsp90 subunits, even in the absence of nucleotides.

An important and unexpected finding, revealed in heterodimer experiments with engineered Hsp90 variants, is that one molecule of Aha1 per Hsp90 dimer is sufficient for maximum acceleration of the ATPase. As there is a greater than 30-fold excess of Hsp90 molecules in the cytosol of *S. cerevisiae* in comparison to Aha1 (Ghaemmaghami et al., 2003), it is likely that a complex consisting of one Aha1 molecule and one Hsp90 dimer is the physiologically relevant species. This stoichiometry has interesting consequences for the mechanism of action of Aha1 in particular and other cochaperones of Hsp90, such as Hop/Sti1 and p23/Sba1, in general, as the expression levels of cochaperones are typically lower compared to Hsp90 (Ghaemmaghami et al., 2003). For Aha1, we have shown that it facilitates the dimerization of the N-terminal domains of Hsp90, and it seems that either rearrangement in one N-terminal domain is sufficient to promote N-terminal dimerization or that one Aha1 can directly bridge and connect the two N-terminal domains. In the scenario in which Aha1 acts in *cis*, Aha1 is only bound to one Hsp90 protomer, stimulating the Hsp90 N-terminal domain to associate

with the N-terminal domain of the other protomer for activation. However, from a sterical point of view, the NMR data suggest that a mechanism in which Aha1 acts as a bridge connecting both N-terminal domains is more likely to reflect the mode of action. The NMR chemical shift changes upon addition of Aha1-C cluster at two sites in Hsp90-N. These sites form a binding groove only when both N domains are dimerized, as observed in the closed Hsp90 structure. These data point toward a mechanism in which Aha1 binds to both N-terminal domains of Hsp90 rather than to just one N-terminal domain. Therefore, the *cis* and *trans* interactions cannot be separated, as they take place simultaneously. These results also point toward a bridging function of Aha1 in which the N- and C-terminal domains of Aha1 interact with different Hsp90 subunits and facilitate their dimerization.

Taken together, our results allow the integration of Aha1 into the Hsp90 cycle (Figure 7). A monomer of Aha1 binds in an asymmetric manner to an Hsp90 dimer in the open conformation. Binding of Aha1 induces changes in the conformation of Hsp90, even in the absence of nucleotides. Presumably, the structure of the N-terminal domain is modulated, and the N-terminal and middle domains of Hsp90 are reoriented toward a closed state ("closed 1"), which then facilitates N-terminal dimerization. This state may reduce the energy barrier between the open and N-terminal dimerized forms of Hsp90. Of interest, the binding of Aha1 leads to a very stable Hsp90 dimer, comparable to the effects determined for a nonhydrolyzable ATP analog (Hessling et al., 2009) and consistent with the idea of a bridging function for Aha1. Binding of ATP to this primed conformation induces association of the Aha1 C domain and the N-terminal domain of Hsp90, and this may further accelerate the formation of the closed conformation competent for ATP hydrolysis ("closed 2").

It is well known that binding and hydrolysis of ATP are essential for the in vivo function of Hsp90 (Obermann et al., 1998; Panaretou et al., 1998) and that the ATP hydrolysis rate is decelerated in the presence of the cochaperones Hop/Sti1 and p23/Sba1 (Johnson et al., 1998; McLaughlin et al., 2006; Richter et al., 2003, 2004). However, the situation in vivo may be more complex, as the different cochaperones are simultaneously present and may influence each other. Our results on the presence of an activating and inhibiting chaperone suggest that ternary complexes are possible and that, in these, the activator Aha1 and either Hop/Sti1 or p23/Sba1 could act on Hsp90 at the same time. They seem to significantly affect each other's influence on Hsp90 activity. These findings are in excellent agreement with an asymmetric activation mechanism of Aha1, which would allow the formation of ternary complexes. However, further studies are required to determine whether asymmetry is important for client protein maturation.

Because substrate binding is thought to occur in the region of the N-terminal and middle domains of Hsp90 (Scheibel et al., 1998; Vaughan et al., 2006), symmetric binding of Aha1 to both the middle and N-terminal domains would potentially block substrate binding. The proposed mechanism allows regulation of the ATPase activity of both subunits in the Hsp90 dimer by Aha1 bound to one subunit and client protein interaction with the second subunit simultaneously, highlighting the potential of an asymmetric activation mechanism.

EXPERIMENTAL PROCEDURES

Protein Production and Purification

The gene of yeast Hsp90 of *S. cerevisiae* was cloned in the vector pET28a (Invitrogen, Karlsruhe, Germany), resulting in an N terminally His_6-tagged protein. QuikChange Site-Directed Mutagenesis was performed according to the manufacturer's protocol (Invitrogen, Karlsruhe, Germany). The PCR fragments of the yeast Aha1 N domain (Aha1-N, residues 1–156) and the Aha1 C domain (Aha1-C, residues 157–356) were cloned in pET28a using *NdeI*/*XhoI*. All constructs were expressed in the *E. coli* strain BL21 (DE3) cod^+ (Stratagene, La Jolla, CA). At an OD_{600} of 0.8, the bacterial cultures were induced with 1 mM isopropyl-1-thio-D-galactopyranoside (IPTG) and shifted to 20°C for overnight expression. Subsequently, proteins were purified according to published protocols (Richter et al., 2001, 2008). N-terminal His_6 tags of Aha1, Aha1 constructs, and Hsp90 domains were cleaved overnight at 4°C using thrombin (25 U/ml) and purified by gel filtration using a Superdex 75 Column (GE Biosciences Europe, Freiburg, Germany). All proteins were stored in 50 mM HEPES/KOH (pH 7.5), 150 mM KCl, and 1 mM TCEP. The purity and the correct molecular mass of all proteins were analyzed by SDS-PAGE and MALDI-TOF. The extinction coefficients used to calculate the protein concentrations were obtained from the ProtParam analysis (http://us.expasy.org/tools/protparam.html).

ATPase Measurements

ATPase assays were performed as described earlier using an ATP regenerating system (Panaretou et al., 1998). In brief, the ATPase activity of 1 to 2.5 μM Hsp90 was measured in 40 mM HEPES/KOH (pH 7.5), 20 mM KCl, 10 mM $MgCl_2$, and 5 mM ATP at 30°C. For subtraction of background ATPase activity, the assay was stopped by the addition of 125 μM radicicol (Sigma, Munich, Germany) to the reaction, and ATPase activity was analyzed using linear regression. Hsp90 cochaperones were added as indicated. Binding affinities were calculated from the data using equation 1:

$$y = \left(\frac{B_{max} \cdot x}{K_{app} + x}\right) + x_0 \quad (1)$$

in which B_{max} is the top asymptote, x_0 is the offset, and K_{app} is the apparent binding affinity.

Heterodimer Assays

To allow equilibration of heterodimers, the samples containing Hsp90 variants were incubated for 5 min at 30°C before adding Aha1. The reaction was started after an additional 5 min by adding ATP. Data analysis relied on the assumption that the binding of mutants to each other is as effective as the binding of mutants to Hsp90 wild-type and homodimerization (Richter et al., 2001).

Subunit Exchange and N-Terminal Dimerization of Hsp90

For FRET measurements, a labeled Hsp90 mutant, yHsp90D61C, was used, which had been shown to be applicable for energy transfer measurements (Hessling et al., 2009). yHsp90D61C was either labeled using ATTO-488-maleimide or ATTO-550-maleimide (Atto-Tec, Siegen, Germany) at room temperature for 2 hr. Free label was quenched with dithiothreitol (DTT) and separated by a desalting column (HiPrep 26/10, GE Biosciences Europe, Freiburg, Germany). The protein was stored in 40 mM HEPES/KOH (pH 7.5) and 20 mM KCl.

Association of FRET Dimers

For dimer formation, 100 nM donor-labeled and 100 nM acceptor-labeled Hsp90 were mixed. Formation of heterodimers containing donor- and acceptor-labeled subunits was followed by monitoring the emergence of a FRET signal.

Association of Aha1 Variants

Aha1 variants were titrated to the mixed Hsp90 heterodimers, and the effect on FRET efficiencies was measured as the decrease in acceptor fluorescence. Aha1 concentration was set to 20 μM, whereas the concentration of the Aha1 domains was set to 60 μM each to enable interaction in their fully saturated range. To determine subunit exchange in the dimer, 10 μM unlabeled

Hsp90 WT was added to the solution, and after a mixing time of 10 s, the decrease in acceptor fluorescence was measured over time at 20°C. To determine the apparent half-life of the subunit exchange reaction, the data for the subunit exchange were qualitatively fit using equation 2:

$$y = y_0 + A \cdot \exp\left(-x / \left(\frac{\ln(2)}{t_{1/2,app}} \right) \right) \quad (2)$$

in which y_0 is the offset, A is the amplitude of fluorescence change, and $t_{1/2,\,app}$ is the apparent half-life of the reaction. The half-life was fit using Origin software (MicroCal, Northampton, MA).

NMR Spectroscopy and Molecular Modeling

To obtain the interaction sites between the proteins involved, ^{15}N-HSQC experiments were used, and the resulting chemical shift differences upon titration of the partner protein to a solution of ^{15}N-labeled protein were analyzed as described (Dehner et al., 2003). For the chemical shift assignments and the structural modeling, see Supplemental Information online.

In brief, to obtain a structural model of the Hsp90-Aha1 complex, we used chemical shift information and existing structures. First, the Aha1 N-terminal domain (PDB:1usu) was aligned to the Hsp90 full-length structure (PDB:1cg9) with PyMOL (DeLano Scientific, Palo Alto, CA, www.pymol.org) and compared with the obtained chemical shift differences of the Hsp90 middle domain and Aha1 (Meyer et al., 2004). Then, the chemical shift changes of the Hsp90 N-terminal domain in the presence of AMP-PNP and the Aha1 C-terminal domain (PDB:1x53) were mapped onto the Hsp90 structure. For the yeast Aha1 C-terminal domain, a homology model was obtained with the program MODELER (Sali and Blundell, 1993) using the NMR structure of the human Aha1 C domain (PDB:1x53). Visualization and figure preparation were done with PyMOL and Chimera (Pettersen et al., 2004).

ACCESSION NUMBERS

The chemical shift assignment of the yeast Aha-C domain was deposited at the BMRB data base under accession code 16588.

SUPPLEMENTAL INFORMATION

Supplemental Information includes Supplemental Experimental Procedures, one table, and five figures and can be found with this article online at doi:10.1016/j.molcel.2010.01.006.

ACKNOWLEDGMENTS

This work was supported by grants of the Deutsche Forschungsgemeinschaft to J.B., K.R., and H.K. and the Fonds der Chemischen Industrie to J.B., K.R., and H.K. M.R. was supported by a fellowship of the Fonds der Chemischen Industrie and F.H. by the ComplNt program of the Elitenetzwerk Bayern.

Received: May 7, 2009
Revised: August 14, 2009
Accepted: December 7, 2009
Published: February 11, 2010

REFERENCES

Ali, M.M.U., Roe, S.M., Vaughan, C.K., Meyer, P., Panaretou, B., Piper, P.W., Prodromou, C., and Pearl, L.H. (2006). Crystal structure of an Hsp90-nucleotide-p23/Sba1 closed chaperone complex. Nature *440*, 1013–1017.

Bukau, B., Weissman, J., and Horwich, A. (2006). Molecular chaperones and protein quality control. Cell *125*, 443–451.

Dehner, A., Furrer, J., Richter, K., Schuster, I., Buchner, J., and Kessler, H. (2003). NMR chemical shift perturbation study of the N-terminal domain of Hsp90 upon binding of ADP, AMP-PNP, geldanamycin, and radicicol. ChemBioChem *4*, 870–877.

Dollins, D.E., Warren, J.J., Immormino, R.M., and Gewirth, D.T. (2007). Structures of GRP94-nucleotide complexes reveal mechanistic differences between the hsp90 chaperones. Mol. Cell *28*, 41–56.

Fan, C.Y., Lee, S., and Cyr, D.M. (2003). Mechanisms for regulation of Hsp70 function by Hsp40. Cell Stress Chaperones *8*, 309–316.

Forafonov, F., Toogun, O.A., Grad, I., Suslova, E., Freeman, B.C., and Picard, D. (2008). p23/Sba1p protects against Hsp90 inhibitors independently of its intrinsic chaperone activity. Mol. Cell. Biol. *28*, 3446–3456.

Geller, R., Vignuzzi, M., Andino, R., and Frydman, J. (2007). Evolutionary constraints on chaperone-mediated folding provide an antiviral approach refractory to development of drug resistance. Genes Dev. *21*, 195–205.

Ghaemmaghami, S., Huh, W.K., Bower, K., Howson, R.W., Belle, A., Dephoure, N., O'Shea, E.K., and Weissman, J.S. (2003). Global analysis of protein expression in yeast. Nature *425*, 737–741.

Graf, C., Stankiewicz, M., Kramer, G., and Mayer, M.P. (2009). Spatially and kinetically resolved changes in the conformational dynamics of the Hsp90 chaperone machine. EMBO J. *28*, 602–613.

Harst, A., Lin, H., and Obermann, W.M. (2005). Aha1 competes with Hop, p50 and p23 for binding to the molecular chaperone Hsp90 and contributes to kinase and hormone receptor activation. Biochem. J. *387*, 789–796.

Hawle, P., Siepmann, M., Harst, A., Siderius, M., Reusch, H.P., and Obermann, W.M. (2006). The middle domain of Hsp90 acts as a discriminator between different types of client proteins. Mol. Cell. Biol. *26*, 8385–8395.

Hessling, M., Richter, K., and Buchner, J. (2009). Dissection of the ATP-induced conformational cycle of the molecular chaperone Hsp90. Nat. Struct. Mol. Biol. *16*, 287–293.

Holmes, J.L., Sharp, S.Y., Hobbs, S., and Workman, P. (2008). Silencing of HSP90 cochaperone AHA1 expression decreases client protein activation and increases cellular sensitivity to the HSP90 inhibitor 17-allylamino-17-demethoxygeldanamycin. Cancer Res. *68*, 1188–1197.

Johnson, J.L., Beito, T.G., Krco, C.J., and Toft, D.O. (1994). Characterization of a novel 23-kilodalton protein of unactive progesterone receptor complexes. Mol. Cell. Biol. *14*, 1956–1963.

Johnson, J., Corbisier, R., Stensgard, B., and Toft, D. (1996). The involvement of p23, hsp90, and immunophilins in the assembly of progesterone receptor complexes. J. Steroid Biochem. Mol. Biol. *56*(*1-6 Spec No*), 31–37.

Johnson, B.D., Schumacher, R.J., Ross, E.D., and Toft, D.O. (1998). Hop modulates Hsp70/Hsp90 interactions in protein folding. J. Biol. Chem. *273*, 3679–3686.

Lotz, G.P., Lin, H., Harst, A., and Obermann, W.M. (2003). Aha1 binds to the middle domain of Hsp90, contributes to client protein activation, and stimulates the ATPase activity of the molecular chaperone. J. Biol. Chem. *278*, 17228–17235.

Martinez-Yamout, M.A., Venkitakrishnan, R.P., Preece, N.E., Kroon, G., Wright, P.E., and Dyson, H.J. (2006). Localization of sites of interaction between p23 and Hsp90 in solution. J. Biol. Chem. *281*, 14457–14464.

McClellan, A.J., Xia, Y., Deutschbauer, A.M., Davis, R.W., Gerstein, M., and Frydman, J. (2007). Diverse cellular functions of the Hsp90 molecular chaperone uncovered using systems approaches. Cell *131*, 121–135.

McLaughlin, S.H., Sobott, F., Yao, Z.P., Zhang, W., Nielsen, P.R., Grossmann, J.G., Laue, E.D., Robinson, C.V., and Jackson, S.E. (2006). The co-chaperone p23 arrests the Hsp90 ATPase cycle to trap client proteins. J. Mol. Biol. *356*, 746–758.

Meyer, P., Prodromou, C., Liao, C., Hu, B., Roe, S.M., Vaughan, C.K., Vlasic, I., Panaretou, B., Piper, P.W., and Pearl, L.H. (2004). Structural basis for recruitment of the ATPase activator Aha1 to the Hsp90 chaperone machinery. EMBO J. *23*, 1402–1410.

Mickler, M., Hessling, M., Ratzke, C., Buchner, J., and Hugel, T. (2009). The large conformational changes of Hsp90 are only weakly coupled to ATP hydrolysis. Nat. Struct. Mol. Biol. *16*, 281–286.

Nathan, D.F., Vos, M.H., and Lindquist, S. (1999). Identification of SSF1, CNS1, and HCH1 as multicopy suppressors of a *Saccharomyces cerevisiae* Hsp90 loss-of-function mutation. Proc. Natl. Acad. Sci. USA *96*, 1409–1414.

Neckers, L., Tsutsumi, S., and Mollapour, M. (2009). Visualizing the twists and turns of a molecular chaperone. Nat. Struct. Mol. Biol. *16*, 235–236.

Obermann, W.M., Sondermann, H., Russo, A.A., Pavletich, N.P., and Hartl, F.U. (1998). In vivo function of Hsp90 is dependent on ATP binding and ATP hydrolysis. J. Cell Biol. *143*, 901–910.

Onuoha, S.C., Coulstock, E.T., Grossmann, J.G., and Jackson, S.E. (2008). Structural studies on the co-chaperone Hop and its complexes with Hsp90. J. Mol. Biol. *379*, 732–744.

Panaretou, B., Prodromou, C., Roe, S.M., O'Brien, R., Ladbury, J.E., Piper, P.W., and Pearl, L.H. (1998). ATP binding and hydrolysis are essential to the function of the Hsp90 molecular chaperone in vivo. EMBO J. *17*, 4829–4836.

Panaretou, B., Siligardi, G., Meyer, P., Maloney, A., Sullivan, J.K., Singh, S., Millson, S.H., Clarke, P.A., Naaby-Hansen, S., Stein, R., et al. (2002). Activation of the ATPase activity of hsp90 by the stress-regulated cochaperone aha1. Mol. Cell *10*, 1307–1318.

Pettersen, E.F., Goddard, T.D., Huang, C.C., Couch, G.S., Greenblatt, D.M., Meng, E.C., and Ferrin, T.E. (2004). UCSF Chimera—a visualization system for exploratory research and analysis. J. Comput. Chem. *25*, 1605–1612.

Picard, D. (2002). Heat-shock protein 90, a chaperone for folding and regulation. Cell. Mol. Life Sci. *59*, 1640–1648.

Pirkl, F., and Buchner, J. (2001). Functional analysis of the Hsp90-associated human peptidyl prolyl cis/trans isomerases FKBP51, FKBP52 and Cyp40. J. Mol. Biol. *308*, 795–806.

Pratt, W.B., and Toft, D.O. (2003). Regulation of signaling protein function and trafficking by the hsp90/hsp70-based chaperone machinery. Exp. Biol. Med. (Maywood) *228*, 111–133.

Prodromou, C., and Pearl, L.H. (2003). Structure and functional relationships of Hsp90. Curr. Cancer Drug Targets *3*, 301–323.

Prodromou, C., Panaretou, B., Chohan, S., Siligardi, G., O'Brien, R., Ladbury, J.E., Roe, S.M., Piper, P.W., and Pearl, L.H. (2000). The ATPase cycle of Hsp90 drives a molecular 'clamp' via transient dimerization of the N-terminal domains. EMBO J. *19*, 4383–4392.

Richter, K., Muschler, P., Hainzl, O., and Buchner, J. (2001). Coordinated ATP hydrolysis by the Hsp90 dimer. J. Biol. Chem. *276*, 33689–33696.

Richter, K., Reinstein, J., and Buchner, J. (2002). N-terminal residues regulate the catalytic efficiency of the Hsp90 ATPase cycle. J. Biol. Chem. *277*, 44905–44910.

Richter, K., Muschler, P., Hainzl, O., Reinstein, J., and Buchner, J. (2003). Sti1 is a non-competitive inhibitor of the Hsp90 ATPase. Binding prevents the N-terminal dimerization reaction during the atpase cycle. J. Biol. Chem. *278*, 10328–10333.

Richter, K., Walter, S., and Buchner, J. (2004). The Co-chaperone Sba1 connects the ATPase reaction of Hsp90 to the progression of the chaperone cycle. J. Mol. Biol. *342*, 1403–1413.

Richter, K., Soroka, J., Skalniak, L., Leskovar, A., Hessling, M., Reinstein, J., and Buchner, J. (2008). Conserved conformational changes in the ATPase cycle of human Hsp90. J. Biol. Chem. *283*, 17757–17765.

Riggs, D.L., Roberts, P.J., Chirillo, S.C., Cheung-Flynn, J., Prapapanich, V., Ratajczak, T., Gaber, R., Picard, D., and Smith, D.F. (2003). The Hsp90-binding peptidylprolyl isomerase FKBP52 potentiates glucocorticoid signaling in vivo. EMBO J. *22*, 1158–1167.

Salek, R.M., Williams, M.A., Prodromou, C., Pearl, L.H., and Ladbury, J.E. (2002). Backbone resonance assignments of the 25kD N-terminal ATPase domain from the Hsp90 chaperone. J. Biomol. NMR *23*, 327–328.

Sali, A., and Blundell, T.L. (1993). Comparative protein modelling by satisfaction of spatial restraints. J. Mol. Biol. *234*, 779–815.

Scheibel, T., Weikl, T., and Buchner, J. (1998). Two chaperone sites in Hsp90 differing in substrate specificity and ATP dependence. Proc. Natl. Acad. Sci. USA *95*, 1495–1499.

Shiau, A.K., Harris, S.F., Southworth, D.R., and Agard, D.A. (2006). Structural Analysis of *E. coli* hsp90 reveals dramatic nucleotide-dependent conformational rearrangements. Cell *127*, 329–340.

Siligardi, G., Hu, B., Panaretou, B., Piper, P.W., Pearl, L.H., and Prodromou, C. (2004). Co-chaperone regulation of conformational switching in the Hsp90 ATPase cycle. J. Biol. Chem. *279*, 51989–51998.

Smith, D.F., Sullivan, W.P., Marion, T.N., Zaitsu, K., Madden, B., McCormick, D.J., and Toft, D.O. (1993). Identification of a 60-kilodalton stress-related protein, p60, which interacts with hsp90 and hsp70. Mol. Cell. Biol. *13*, 869–876.

Sullivan, W.P., Owen, B.A., and Toft, D.O. (2002). The influence of ATP and p23 on the conformation of hsp90. J. Biol. Chem. *277*, 45942–45948.

Vaughan, C.K., Gohlke, U., Sobott, F., Good, V.M., Ali, M.M., Prodromou, C., Robinson, C.V., Saibil, H.R., and Pearl, L.H. (2006). Structure of an Hsp90-Cdc37-Cdk4 complex. Mol. Cell *23*, 697–707.

Wandinger, S.K., Suhre, M.H., Wegele, H., and Buchner, J. (2006). The phosphatase Ppt1 is a dedicated regulator of the molecular chaperone Hsp90. EMBO J. *25*, 367–376.

Wang, X., Venable, J., LaPointe, P., Hutt, D.M., Koulov, A.V., Coppinger, J., Gurkan, C., Kellner, W., Matteson, J., Plutner, H., et al. (2006). Hsp90 cochaperone Aha1 downregulation rescues misfolding of CFTR in cystic fibrosis. Cell *127*, 803–815.

Xu, W., Yuan, X., Xiang, Z., Mimnaugh, E., Marcu, M., and Neckers, L. (2005). Surface charge and hydrophobicity determine ErbB2 binding to the Hsp90 chaperone complex. Nat. Struct. Mol. Biol. *12*, 120–126.